microplastics

MDPI

Article

Health Risks of Pristine and Leached Polystyrene Micro- and Nanoplastics: An In Vitro Study on Human Dental Pulp Stem Cells

Ludovica Barone [1], Federica Rossi [1], Marina Borgese [2], Maria Maisano [3], Tiziana Cappello [3], Mario Raspanti [2], Christina Pagiatakis [1,4], Roberto Papait [1,4], Giovanni Bernardini [1] and Rosalba Gornati [1,*]

[1] Department of Biotechnology and Life Sciences, University of Insubria, 21100 Varese, Italy; ludovica.barone@uninsubria.it (L.B.); federica.rossi@uninsubria.it (F.R.); christina.pagiatakis@uninsubria.it (C.P.); roberto.papait@uninsubria.it (R.P.); giovanni.bernardini@uninsubria.it (G.B.)
[2] Department of Medicine and Technological Innovation, University of Insubria, 21100 Varese, Italy; marina.borgese@uninsubria.it (M.B.); mario.raspanti@uninsubria.it (M.R.)
[3] Department of Chemical, Biological, Pharmaceutical and Environmental Sciences, University of Messina, 98166 Messina, Italy; mmaisano@unime.it (M.M.); tiziana.cappello@unime.it (T.C.)
[4] Department of Cardiovascular Medicine, IRCCS Humanitas Research Hospital, Rozzano, 20089 Milan, Italy
* Correspondence: rosalba.gornati@uninsubria.it; Tel.: +39-0332421314

Abstract

The toxicity of micro- and nanoplastics in aquatic life is well documented, yet limited information is available on their effects in humans; moreover, most in vitro nanotoxicology studies rely on cancer cells. This study examined the effects of pristine and aged polystyrene micro- and nanoparticles on human dental pulp stem cells. While both particle sizes were internalized by the cells, primarily through endocytosis, they did not affect cell viability. In contrast, leachates from particles, aged for one month in culture medium, significantly reduced viability, indicating that toxicity arises from degradation byproducts rather than the particles themselves. Atomic force microscopy confirmed surface changes in aged plastics. Both particle sizes disorganized the cytoskeleton, leading to reduced actomyosin cortex integrity. Gene expression analysis revealed that leachates and aged particles activated inflammatory pathways, markedly increasing IL-8 and TGF-β1 expression, while also decreasing SOD levels associated with oxidative stress. No notable effects were observed on genes related to stemness or senescence. These results suggest that, while pristine micro- and nanoplastics may be relatively inert, their degradation products pose greater toxicological risks to human health. The findings highlight the importance of considering leachate toxicity in plastic pollution studies and demonstrate the value of stem cell-based models for evaluating the cellular and molecular impacts of environmental contaminants on human health.

Keywords: nanotoxicology; polystyrene; aged plastic; mesenchymal stem cells

Academic Editor: Piotr Zieliński

Received: 14 November 2025
Revised: 16 December 2025
Accepted: 9 January 2026
Published: 3 February 2026

1. Introduction

Polystyrene (PS) is one of the most widely used plastic polymers in the world and a major component of plastic debris commonly released into the ecosystem. In the natural environment, plastics are difficult to break down due to their hydrophobicity, the presence of persistent covalent bonds, and their functional groups' resistance to chemical–physical attack [1]. However, the long-term influence of environmental factors such as ultraviolet

(UV) radiation, temperature, and wave action breaks down large plastic pieces into smaller ones that, because of their persistence, can cause harmful impacts and become an important environmental issue of global concern [2,3].

According to their size, pieces of plastic debris are classified as macro (>5 mm), micro (in the 100 nm to 5 mm range) and nano (<100 nm) particles [4–6]. The macro particles can tangle around animal bodies or be ingested, causing their death due to digestive tract clogs. It has been estimated that over 1 million animals, especially those that populate the aquatic environment, are killed every year due to macro plastic pollution [7,8].

According to their origin, micro- and nanoplastics can be classified as primary and secondary. The primary particles are those intentionally manufactured as components of consumer products (scrubs, soaps, cleansers, toothpastes, fast food containers, and biomedical devices) and do not represent a significant mass-based fraction of exposure. The secondary plastics result from the fragmentation of larger materials by degradation [7,9–11]. The high surface curvature and surface-to-volume ratio of nanoplastics influence their physicochemical properties such as hydrophily, surface charge, and chemistry, making them a potentially great ecological problem. Moreover, due to their dimensions, NP can be internalized by cells and accumulate further along the food chain [1,2,7].

As about 71% of the earth's surface is occupied by water (oceans 97%, while ponds, streams, glaciers, and ice caps account for 3%), it is not surprising that the impact of microplastics and nanoplastics on aquatic habitats is well-documented by extensive reviews [7,12–14], reports [15], or guides to develop suitable monitoring strategies [16].

Conversely, little is known about the effects of microplastics and nanoplastics on terrestrial species, and, due to lack of evidence, the results of their toxicity at the cellular level are still controversial [10,17–19]. For this reason, in this study, we have investigated the cytotoxicity of both pristine and leached polystyrene microplastics ($PS_{1\ \mu m}$) and nanoplastics ($PS_{100\ nm}$) using human Dental Pulp Stem Cells (DPSCs) as a cell model.

DPSCs are a subpopulation of Mesenchymal Stem Cells (MSCs) embedded within the pulp cavity of teeth. Due to its anatomical location, abundant sensory innervation, and rich micro circular network, dental pulp represents a unique tissue easily invaded from exogenous compounds including those released by chewing gums, such as polyethylene and polypropylene (https://www.acs.org/pressroom/presspacs/2025 accessed on 16 October 2025), and those delivered by teeth aligners composed of transparent resin of various natures [20,21]. DPSCs are characterized by high proliferation rate and stemness features compared to other types of MSCs; furthermore, dental pulp, obtained from the removal of impacted third molars, is considered surgical waste material [22–24]. All these characteristics make DPSCs an excellent model for toxicity studies on stem cells. It is important to consider that stem cells, present in all human tissues including neural tissue, are fundamental for maintaining homeostasis and remodeling healthy tissues over the course of a lifetime. In addition, as they are also involved in tissue repair, they possess great potential in many medical applications, such as regenerative medicine, bone marrow transplantation, orthopedic injuries, and autoimmune, cardiovascular, and liver diseases [25,26].

It is, therefore, evident how dangerous it could be to perturb stem cell equilibrium. This may lead to their depletion, which, in turn, is responsible for pathological consequences.

The aim of this study is to evaluate the cytotoxicity of PS particles, the cellular uptake and cytoskeleton organization following exposure, and the changes in gene expression related to oxidative stress, inflammation, stemness, and senescence in DPSCs. Given the growing evidence that chemical compounds leached from micro- and nanoplastics exert significant biological effects, this study investigates the impact of both pristine PS particles and leachates from PS particles that mimic their persistence in the human body. Notably, the release of material from particles is not limited to plastics; even metal nanoparticles, which

are generally considered stable, can release components (i.e., ions) when placed in aqueous systems, such as saline solutions, cell culture media, or the tissue microenvironment [27–29].

The results of this research aim to provide new insights into the potential risks that plastics and their leachates pose to human health when they come into contact with human stem cells.

2. Materials and Methods

2.1. Chemicals and Plastics

Chemicals were purchased from Merck (Milano, Italy), Promega (Milano, Italy), Zymo Research (Milano, Italy), BioRad (Milano, Italy), Invitrogen, and Life Technologies (Milano, Italy), unless otherwise indicated.

Polybead® Microspheres 1.00 µm ($PS_{1\ \mu m}$) and 0.10 µm ($PS_{100\ nm}$) were purchased from Polyscience Inc. (Niles, IL, USA).

For all experiments, we chose to use the same concentration of PS, even though this implied using a different number of particles (a 10^3-fold difference between micro- and nanoplastics).

2.2. Plastic Characterization

Shape and morphology were investigated by Zeiss Gemini SEM 360 (Oberkochen, Germany) and AFM (Santa Barbara, CA, USA).

For SEM analysis, $PS_{1\ \mu m}$ and $PS_{100\ nm}$ were ultra-centrifugated at 600,000× *g* in a centrifuge tube (Ultra-Clear™, Beckman Coulter, Milano, Italy). Supernatants were removed and samples were resuspended in 0.5 mL of EtOH and then deposited on cover glasses. Samples were left to air dry and were then mounted on appropriate stubs using colloidal silver glue, gold-coated in an Emitech K550 sputter coater (Emitech, Beaucouzé, France) and observed with an FEI XL-30 FEG high-resolution SEM (now Thermo Fisher, Waltham, MA, USA), operated at 2 kV.

For AFM analysis, samples were spun down at 600,000× *g* in an Ultra-Clear™ centrifuge tube (Beckman Coulter, Milano, Italy). Subsequently, 100 µL of each sample were collected and deposited onto the stub previously covered with a virgin mica disk to ensure that the observation of artifacts was avoided; before observation, the samples were left to air dry for a few minutes.

A Nanoscope IIIa (Digital Instruments, Santa Barbara, CA, USA) was utilized for AFM analysis, and the surface characteristics were examined using Gwyddion v.2.61 software (Czech Metrology Institute, Brno, Czech Republic). Images were acquired in tapping mode using a 10 × 10 µm, 5 × 5 µm, and 3 × 3 µm scanning fields.

2.3. Institutional Review Board Statement

Dental pulp-derived mesenchymal stem cells (DPSCs) were isolated from dental pulp tissues of a healthy subject (female 12 years old), undergoing third molar extraction. The subject provided informed consent to be included in the study, which was approved by the institutional review board ethics committees.

The study was conducted according to the guidelines of the Declaration of Helsinki, and approved by the Institutional Ethics Committee of "Ospedale di Circolo Fondazione Macchi" (Protocol number: 0034066, approval date: 3 October 2013).

Consent was obtained from the subject's legal guardians involved in the study.

2.4. Cell Isolation and Maintenance

The dental pulp was digested through collagenase type II at 37 °C for 1 h, under agitation. The obtained fraction was filtered (70 µm-cell strainers) and centrifuged at

256× *g* for 10 min (Neya 8-Remi Elektrotechnik Ltd., Mumbai, India); the resulting pellet was then cultured in T25 flasks at 37 °C, 5% CO_2, in DMEM:DMEM F12 1:1 supplemented with 2 mM ultra-stable L-Gln, 1% penicillin–streptomycin, 0.1% gentamicin, and 10% fetal bovine serum (FBS). After 24 h, unattached cells were removed. The cells were expanded into T75 flasks and used for all the experiments at the fifth passage. Characterization of DPSCs was reported in Barone et al. [23].

2.5. Cell Viability Assay

The plastic amounts used in these experiments were based on those reported in the literature [30–34].

Five thousand cells were seeded into a 96-well plate, cultivated for 24 h at 37 °C in 5% of CO_2, and then exposed at increasing amounts of $PS_{1\ \mu m}$ and $PS_{100\ nm}$ (1–1000 µg/mL). In parallel, a negative control (0 µg/mL) was arranged. After exposure (30, 60, 90 min, and 24, 48, 72 h), the plates were equilibrated at RT for 30 min and CellTiter-Glo® Luminescent Cell Viability Assay was conducted according to the manufacturer's instructions. To adopt the most suitable assay, an estimation of interference was previously performed. CellTiter-Glo is based on the luciferase reaction to quantify the amount of ATP present in the cells; the luminescent signal is directly proportional to the number of viable cells. The plate was stirred for 2 min and left at RT for 10 min before detecting the luminescence using the GloMax® Discover Microplate Reader (Promega, Milano, Italy). Three independent experiments, run in triplicate, were conducted for each assay.

2.6. Aging of PS Particles in Culture Medium and Atomic Force Microscopy (AFM) Inspection

$PS_{1\ \mu m}$ and $PS_{100\ nm}$, at a concentration of 1 mg/mL, were maintained in 10 mL of complete culture medium (DMEM:DMEM/F12 1:1, supplemented with 10% FBS) for one month at 37 °C and 5% CO_2 (aged particles). After incubation, the particles were separated from the medium (here referred to as the dissolution medium) by ultracentrifugation at 600,000× *g* (Ultra-Clear™, Beckman Coulter). A cell viability assay was performed by exposing cells to 100 µL of the dissolution medium or to 1 mg/mL of "aged particles" ($PS_{1\ \mu m}$ and $PS_{100\ nm}$) for 30, 60, and 90 min, and 24, 48, and 72 h. The assay was carried out using the same method described in Section 2.5 "Cell Viability Assay", with the addition of an "aged control" consisting of complete medium maintained for one month at 37 °C and 5% CO_2, without plastic particles. Three independent experiments, run in triplicate, were conducted for each assay.

For AFM inspection, 1 mg of pristine and aged PS particles were spun down at 600,000× *g* (Ultra-Clear™, Beckman Coulter). Supernatant was removed and samples were resuspended in 1 mL of milliQ water, then mounted onto the AFM stub, and processed as described in Section 2.2 "Plastic characterization".

2.7. Cellular Uptake and Cytoskeleton Organization

Five thousand cells were seeded in a 48 multiwell and exposed to different concentrations (1–1000 µg/mL) of $PS_{1\ \mu m}$ and $PS_{100\ nm}$. Pictures of the same field were acquired at 30, 60 and 90 min for short-term exposure, and 24, 48 and 72 h for medium-term exposure by contrast phase microscopy.

For SEM observation, 2500 cells were seeded on cover slips in a 24 multiwell and, 24 h later, exposed to different concentrations (1–1000 µg/mL) of $PS_{1\ \mu m}$ and $PS_{100\ nm}$ for 90 min and 72 h. The samples were washed in PBS and fixed in 1% Karnowsky solution in 0.1 M sodium cacodylate buffer (pH 7.4) for 30 min. Afterwards, samples were washed in 0.1 M sodium cacodylate buffer (pH 7.4) and post-fixed for 15 min in 1% osmium tetroxide solution, and subsequently dehydrated through a graded EtOH

series and hexamethyldisilazane. Each sample was then mounted on carbon-coated stubs, gold-coated, and observed as described in the "Plastic characterization" paragraph.

To evaluate cytoskeleton organization, the F-actin filament phalloidin-staining was used. Two thousand five hundred cells were seeded on cover slips, in a 24 multiwell plate, and exposed to 100 µg/mL of $PS_{1\ \mu m}$ and $PS_{100\ nm}$ for 90 min and 72 h. The samples were washed with PBS, fixed with 4% paraformaldehyde (PFA) for 10 min, washed again with PBS and then incubated for 30 min with 2% Bovine Serum Albumin/0.1% Tween-20. Incubation with Alexa Fluor™ 488 phalloidin diluted 1:400 for 60 min was followed by 5 min incubation with 4′,6-diamidino-2-fenilindolo (DAPI, diluted 1:1000 in PBS). To rule out the potential PS autofluorescence, a sample was stained with DAPI only. Samples were then mounted on glass slides and observed with a fluorescence microscope (Axiophot, Carl Zeiss, TiEsselab, Milano, Italy). Phase contrast and fluorescent images were taken using a CCD camera (Discovery C30, TiEsselab, Milano, Italy).

2.8. Study of Endocytic Pathway

To assess particle uptake, inhibition of the endocytic pathway was investigated following the procedure of Mäger et al. [35], with modifications introduced in our laboratory. Briefly, 2500 cells were seeded on a cover glass; after 24 h temperature was lowered to 4 °C to block the endocytosis, and, after 30 min, cells were exposed to 100 µg/mL of $PS_{1\ \mu m}$ or $PS_{100\ nm}$ for 3 h. At the end of the treatments, samples were washed three times in PBS and fixed in 4% PFA for 10 min; images were acquired by phase contrast microscopy using a CCD camera (Discovery C30, TiEsselab, Milano, Italy). In parallel, another set of exposed cells were processed for SEM observation, as reported above.

Furthermore, the uptake blockage was also conducted at 37 °C in the presence of cytochalasin D. For this purpose, cells were seeded as described above, incubated with 4 µM cytochalasin D and later exposed to 100 µg/mL of $PS_{1\ \mu m}$ or $PS_{100\ nm}$ for 3 h, in the presence of 4 µM cytochalasin D. Samples were then fixed and processed for SEM observation.

2.9. RNA Extraction and Gene Expression

Cells were seeded in Petri dishes (10 cm diameter) and, once 80% of confluence was reached, exposed at 10 and 100 µg/mL of $PS_{1\ \mu m}$ and $PS_{100\ nm}$ for 90 min and 72 h; cells were then collected, and total RNA was isolated using the MiniPrep kit (Zymo Research, Freiburg, Germany) according to the manufacturer's protocol.

The extracted RNA was quantified using the QuantiFluor® RNA System and assessed by 1% gel electrophoresis to verify the integrity. The RNA was reverse transcribed using the iScript™ cDNA Synthesis Kit and the cDNA was stored at −20 °C until use. qPCR was conducted using iTaqTM Universal SYBR® Green Supermix. The Beacon Designer Program (BioRad, Milano, Italy) was used to design specific primers, whose sequences are shown in Table 1. Each sample was prepared as reported in Rossi et al. [36]. Briefly, 1 µL (5 ng) of cDNA, 1 µL of forward and reverse primer mix (6 µM), 7.5 µL of SYBR Green Supermix (2×), and a final volume of 15 µL of water were mixed and placed in the CFX 96 Thermocycler (BioRad, Milano, Italy). Gene expression was normalized using β-actin and glyceraldehyde-3-phosphate dehydrogenase (GAPDH) as reference genes [31] and quantified by using the 1/ΔCt method. Three independent experiments, run in duplicate, were conducted for each assay.

The same experiment was performed exposing the cells, for 90 min and 72 h, to 1 mg/mL of "aged particles" ($PS_{1\ \mu m}$ and $PS_{100\ nm}$) and their dissolution media, prepared as described in Section 2.6 "Aging of PS particles in culture medium and Atomic Force Microscopy (AFM) inspection".

Table 1. Primers used in this work.

Gene Name	Primer Sequence 5′-3′	Melting Temperature (°C)	Accession Number
βactin	[1]Fw: GAAGATCAAGATCATTGCTCCTC [2]Rev: GACTCGTCATACTCCTGCTT	63.1 63.1	NM_001101.5
GAPDH	[1]Fw: ATCATCAGCAATGCCTCCT [2]Rev: GAGTCCTTCCACGATACCAA	60.9 60.5	M17851.1
Interleukin-1β (IL-1β)	[1]Fw: CTACGAATCTCCGACCAC [2]Rev: AACCAGCATCTTCCTCAG	60.7 60.5	AY137079.1
Interleukin-6 (IL-6)	[1]Fw: ACTCACCTCTTCAGAACG [2]Rev: CCTCTTTGCTGCTTTCAC	60.0 60.4	M54894.1
Interleukin-8 (IL-8)	[1]Fw: GCCAAGGAGTGCTAAAGA [2]Rev: TGGTCCACTCTCAATCAC	60.8 60.0	M28130.1
Transforming Growth Factor β1 (TGF-β1)	[1]Fw: CTACTACGCCAAGGAGGTC [2]Rev: CTCTGCTTGAACTTGTCATAGATT	63.1 62.9	NM_000660.7
Tumor necrosis factor α (TNF-α)	[1]Fw: AATGGCGTGGAGCTGAGA [2]Rev: TGAAGAGGACCTGGGAGTAGAT	65.3 65.8	M16441.1
Superoxide dismutase (SOD)	[1]Fw: CAGATGACTTGGGCAAAG [2]Rev: CCAATTACACCACAAGCC	59.8 60.1	EF151142.1
Catalase (CAT)	[1]Fw: TACCCTCTCATCCCAGTT [2]Rev: GGTCGAAGGCTATCTGTT	60.4 60.2	AY028632.1
CD44	[1]Fw: GCAGTCAACAGTCGAAGAAG [2]Rev: GTCCTCCACAGCTCCATT	62.9 62.9	AY101192.1
CD90	[1]Fw: CTCTACTTATCCGCCTTCACT [2]Rev: CGTTCTGGGAGGAGATGG	62.9 63.0	NM_006288.5
Dentin Sialophosphoprotein (DSPP)	[1]Fw: GCAGTGACAGTGATAGTAGTG [2]Rev: TTGCTGCTGTCTGACTTG	63.2 63.2	NM_014208.3
Alkaline Phosphatase (ALPL)	[1]Fw: TGAGTGACACAGACAAGAAG [2]Rev: CTGGTAGTTGTTGTGAGCATA	62.6 63.1	AH005272.2
Cyclin-dependent kinase inhibitor 2A (p16)	[1]Fw: CTTCCTGGACACGCTGGTG [2]Rev: ATGGTTACTGCCTCTGGTGC	67.1 66.5	NM_000077.5
Cyclin Dependent Kinase Inhibitor 1A (p21)	[1]Fw: ACCTCACCTGCTCTGCTG [2]Rev: AGGCACAAGGGTACAAGAC	65.6 63.5	NM_000389.5

[1]Fw = Forward primer; [2]Rev = Reverse primer.

2.10. Statistical Analysis

Statistical analysis was conducted using the GraphPad Prism software v10 (GraphPad Prism Inc., San Diego, CA, USA). The ANOVA, followed by Dunnett's multiple comparisons test, was performed and statistical significance was fixed as follows: * $p < 0.01$, ** $p < 0.001$.

3. Results

3.1. Study Design

DPSCs, isolated according to the Gronthos protocol [37] and modified in our laboratory [22], were exposed, for different times, to increasing amounts (1–1000 μg/mL) of $PS_{1\ \mu m}$ and $PS_{100\ nm}$. Toxicity, uptake, cytoskeleton organization, modulation of genes involved in oxidative stress, inflammation, stemness, and senescence caused by $PS_{1\ \mu m}$ and $PS_{100\ nm}$ were evaluated by microscopy and molecular techniques.

3.2. PS Pristine Particle Characterization

PS micro- and nanoparticles were purchased and characterized by Polyscience Inc. (https://www.polysciences.com/german/polybead-microspheres-010956m. accessed on 3

September 2024). According to the manufacturer, Polybead® Microspheres are provided as 2.5% solids (w/v) aqueous suspensions, with a coefficient of variance (CV) of 15%. $PS_{1\ \mu m}$ contains 4.55×10^9 particles/mL, while $PS_{100\ nm}$ contains 4.55×10^{12} particles/mL. The non-functionalized PS microparticles have a weak negative surface charge, with a zeta potential ranging between −10 and −30 mV in distilled water and neutral pH buffer. We complemented the characterization with SEM analysis, and the results are shown in Figure 1.

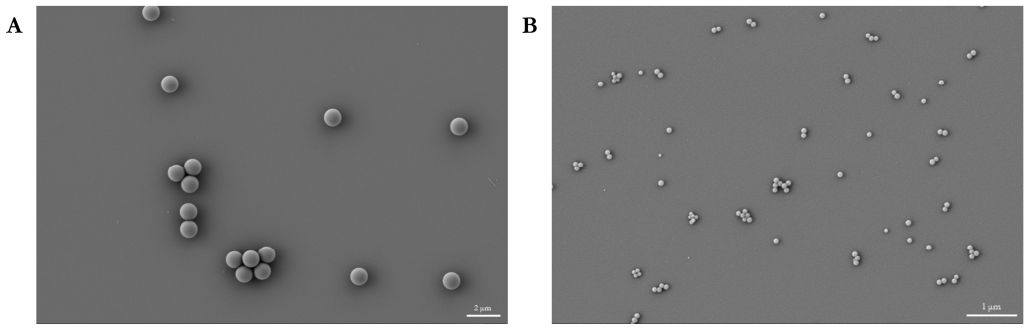

Figure 1. Scanning microscopy image of polystyrene. (**A**): $PS_{1\ \mu m}$, (**B**): $PS_{100\ nm}$; for both particles, size and dimension were confirmed. Scale bars: 2 µm (**A**); 1 µm (**B**).

3.3. Effect of PS Pristine Particles on Cell Viability

To choose the most suitable assay, an estimation of interferences was previously performed and then the CellTiter-Glo® Luminescent Cell Viability Assay was adopted.

As shown in Figure 2, exposure to $PS_{1\ \mu m}$ and $PS_{100\ nm}$ did not cause any significant modification of Relative Luminescent Units (RLU), which are correlated with ATP content, in DPSCs after short- (Figure 2A) and medium-term exposure (Figure 2B) at the chosen concentrations.

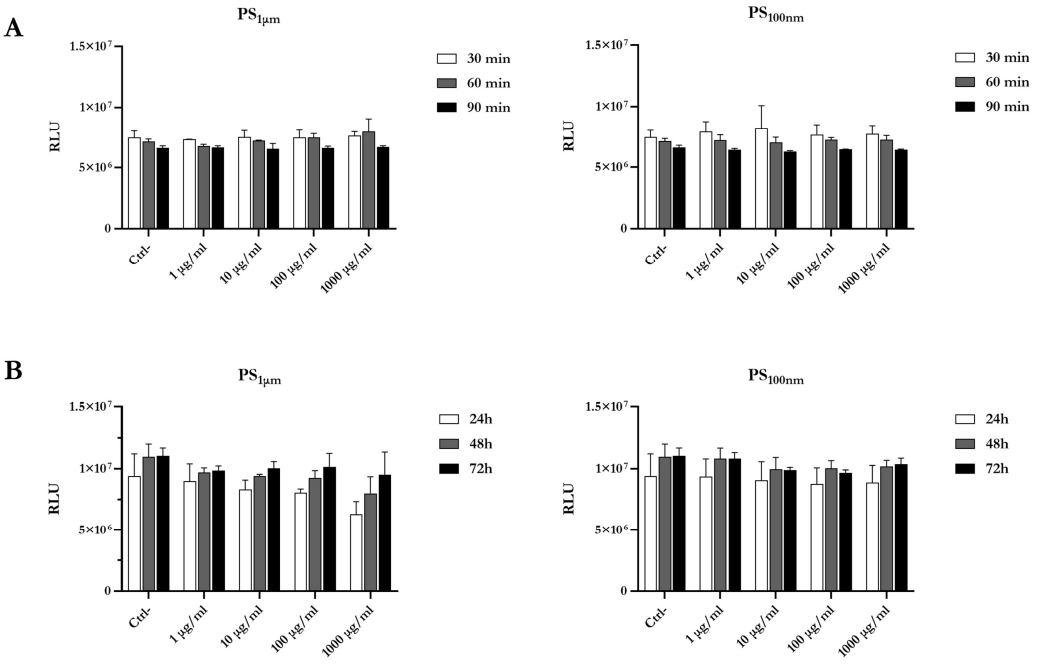

Figure 2. Cell viability. (**A**): short-term exposure to increasing concentrations of $PS_{1\ \mu m}$ and $PS_{100\ nm}$; (**B**): medium-term exposure to increasing concentrations of $PS_{1\ \mu m}$ and $PS_{100\ nm}$. In these experimental conditions, no relevant effects were noticed. Ctrl-: negative control (0 µg/mL). Each assay was run in triplicate and repeated in three independent experiments.

3.4. Effect of Aged PS Particles on Cell Viability

The results shown in Figure 3A indicate that both PS particles, aged for a month in culture medium, and their dissolution medium did not display relevant modifications on cell viability after short-term exposure. Differently, the dissolution medium significantly affected the exposed cells during medium-term treatments (Figure 3B). Unexpectedly, after 72 h of exposure, $PS_{1\ \mu m}$ induces a significant increase in ATP content. No appreciable effects on viability were detected in cells cultured in aged medium. In addition, viability was not affected in cells exposed to PS particles aged for one week in culture medium (Supplementary Materials, Figure S1).

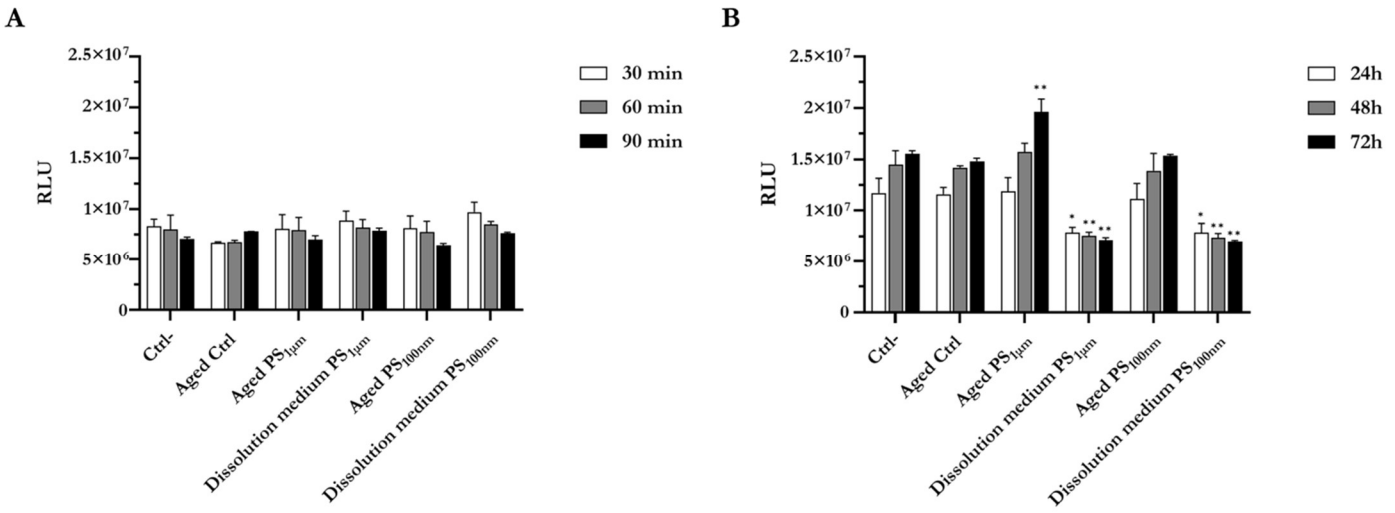

Figure 3. Cell viability response to aged $PS_{1\ \mu m}$, $PS_{100\ nm}$, and dissolution medium obtained after aging of the particles for a month in culture medium. (**A**): short-term exposure; (**B**): medium-term exposure. In these experimental conditions, a reduction of Relative Luminescence Units, correlated with the ATP content, was observed. * $p < 0.01$; ** $p < 0.001$. Ctrl-: negative control; Aged Ctrl: aged control.

3.5. Effect of Aging on PS Particle Surface Evaluated by Atomic Force Microscopy

The surface characteristics of $PS_{1\ \mu m}$ and $PS_{100\ nm}$ showed differences before and after their maintenance for a month in complete culture medium (Figure 4). Particularly, as also reported in Figure 1, pristine particles appear arranged in an orderly manner and stiff (see Figure 4A,C). After a month in complete culture medium, even though the particles did not change their diameter, they appear more clustered, overlapped, mushy, and sticky (see Figure 4B,D). No changes were observed on particles maintained in culture medium for a week (Supplementary Materials, Figure S2).

The changes of particle characteristics described above are the expression of the leaching, and they are in agreement with the onset of cytotoxicity caused by the components leached in the complete culture medium. We cannot exclude, however, the possibility that the surface modifications were due to the formation of a protein corona resulting from the serum present in the culture medium.

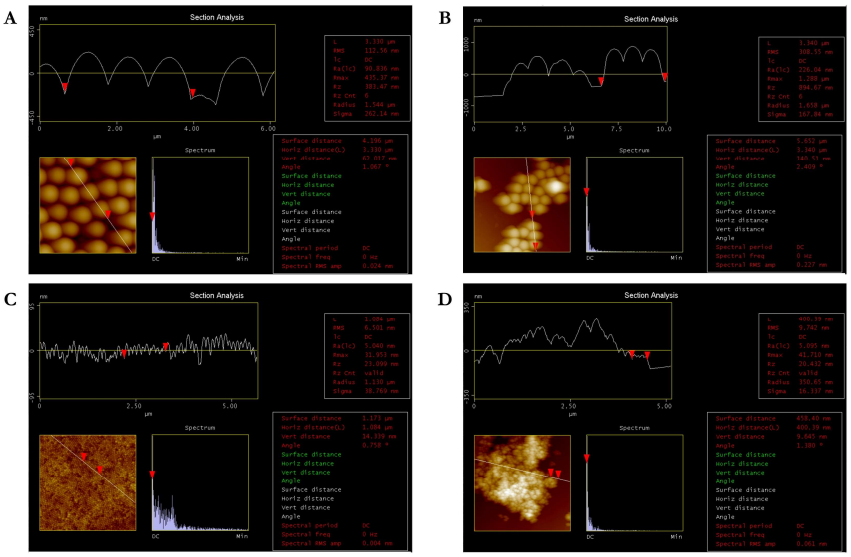

Figure 4. AFM images of PS surfaces. (**A**): $PS_{1\ \mu m}$ before aging, (**C**): $PS_{1\ \mu m}$ after aging for a month in cell medium, (**B**): $PS_{100\ nm}$ before aging, (**D**): $PS_{100\ nm}$ after aging of the particles for a month in cell medium. Aged particles did not change their diameter, however appeared more clustered, overlapped, mushy, and sticky.

3.6. Impact of PS Particles on Cellular Uptake and Cytoskeleton Organization

As illustrated in Figure 5, the cellular uptake is clearly dose- and time-dependent both for $PS_{1\ \mu m}$ and $PS_{100\ nm}$. Already at 90 min of exposure, it was evident that the particles, particularly $PS_{1\ \mu m}$ at the concentration of 1 mg/mL, were massively accumulated close to the cells (Figure 5A). On the other hand, at this exposure time no $PS_{100\ nm}$ were perceived (Figure. 5C). After 72 h, both $PS_{1\ \mu m}$ at the concentration of 100 µg/mL (Figure 5B) and $PS_{100\ nm}$ at the concentration of 1 mg/mL (Figure 5D), were noticeable inside the cells.

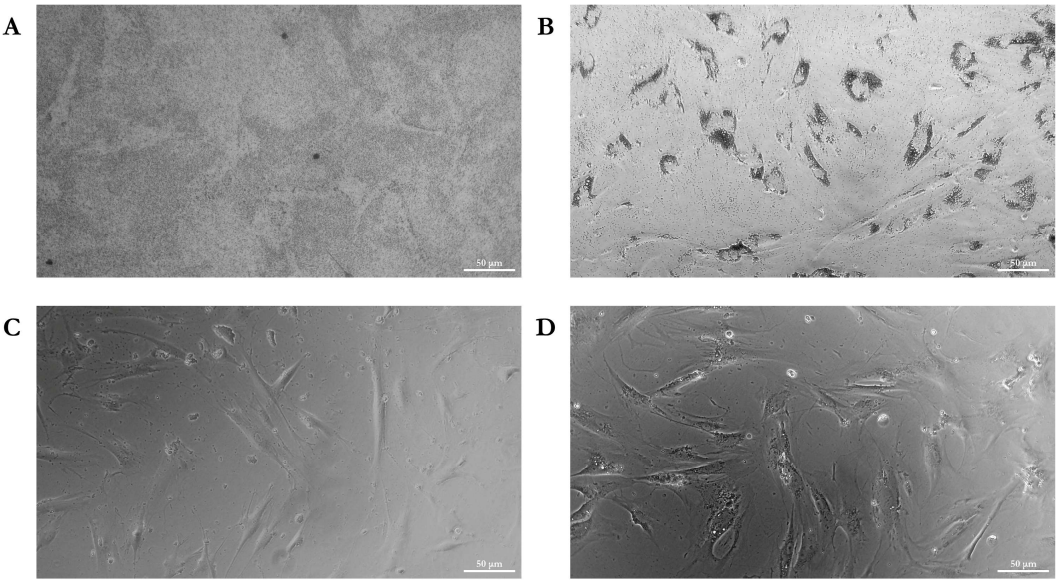

Figure 5. Representative phase contrast microscopy images of DPSCs exposed to PS particles. (**A**): after 90 min of exposure to 1 mg/mL $PS_{1\ \mu m}$, particles were visible as dark shadows around the cells. (**B**): after 72 h of exposure to 100 µg/mL of $PS_{1\ \mu m}$, the particles were massively accumulated in the cytoplasm; (**C**): after 90 min of exposure to 1 mg/mL $PS_{100\ nm}$, extracellular aggregates were observed; (**D**): conversely, after 72 h of exposure to 100 µg/mL of $PS_{100\ nm}$, particles were noticeable inside the cell's cytoplasm. Scale bar 50 µm.

As displayed in Figure 6, SEM analysis corroborated the optical microscopy results. In panels B,C, $PS_{1\ \mu m}$ localized outside the cell were clearly distinguished from the internalized ones due to the black shadow around them. The same consideration was also valid for $PS_{100\ nm}$ (see Figure 6F). Moreover, Figure 6E suggests that internalized particles remain in the cytoplasm.

As illustrated in Figure 7, unexposed cells showed an undisturbed cytoskeleton organization characterized by a dense mesh under the cellular membrane, referring to actomyosin cortex complex (Figure 7A). Differently, β-actin filaments were remodeled in response to $PS_{1\ \mu m}$ and $PS_{100\ nm}$ (Figure 7B,C). In particular, we noticed a decrease in actomyosin cortex complex and an increment of irregular and granular phalloidin staining, a sign of impaired actin polymerization.

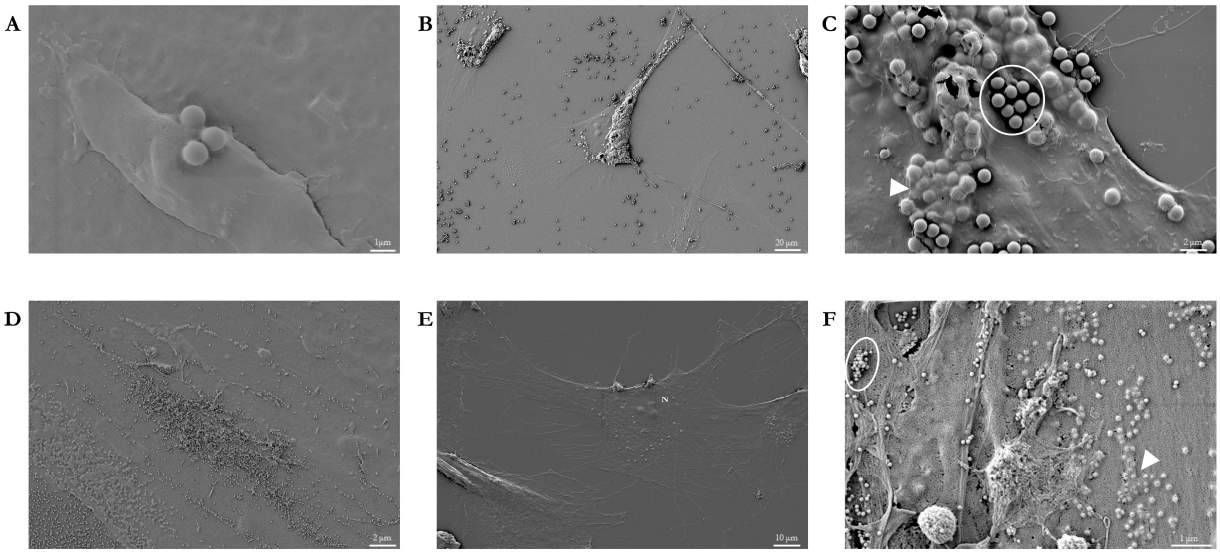

Figure 6. Representative SEM images of DPSCs exposed to PS particles. (**A**): 10 μg/mL $PS_{1\ \mu m}$ for 90 min. (**B**): 100 μg/mL $PS_{1\ \mu m}$ for 72 h; (**C**): 10 μg/mL PS1 μm for 72 h; (**D**): 1 mg/mL $PS_{100\ nm}$ for 90 min; (**E**): 100 μg/mL PS100 nm for 72 h; (**F**): 1 mg/mL $PS_{100\ nm}$ for 72 h. As clearly shown in panel (**C**,**F**), internalized particles (arrowhead) were undoubtedly distinguished from those present outside the cells (circle) due to the black shadow surrounding the last ones. Panel (**E**) suggested that the internalized particles remain in the cytoplasm; N: nucleus. Scale bar 1 μm (**A**,**F**); 2 μm (**C**,**D**); 10 μm (**E**); 20 μm (**B**).

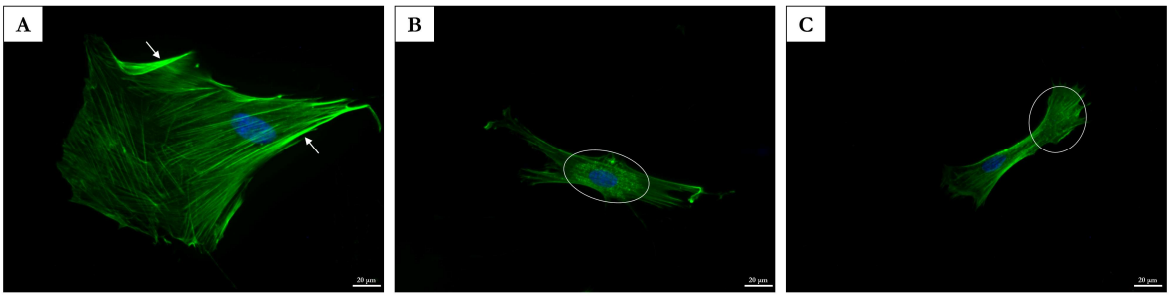

Figure 7. Representative images of fluorescence microscopy of β-actin filament phalloidin-stained (green). (**A**): unexposed cells; (**B**): cells exposed to $PS_{1\ \mu m}$; (**C**): cells exposed to $PS_{100\ nm}$. In these experimental conditions β-actin filaments were remodeled in response to $PS_{1\ \mu m}$ and $PS_{100\ nm}$ exposure. Arrows indicate actomyosin complexes; circles indicate unpolymerized G-actin; nuclei were stained with DAPI. Scale bar 20 μm.

3.7. Study of Cell Uptake Pathway After Exposure to PS Particles

As undoubtedly displayed in Figure 8, when endocytosis is blocked, maintaining cells at 4 °C (Figure 8A–F), or at 37 °C in the presence of 4 µm cytochalasin (Figure 8G–I), we did not see a detectable presence of plastic particles inside the cells. Images were acquired by phase contrast and scanning electron microscopes (SEM). In addition, as reported in Figure 8G–I, the cells treated with cytochalasin, aside from not internalizing the plastic particles, showed a round shape instead of fibroblast-like, and had a reduced adhesion compared to those maintained a 4 °C.

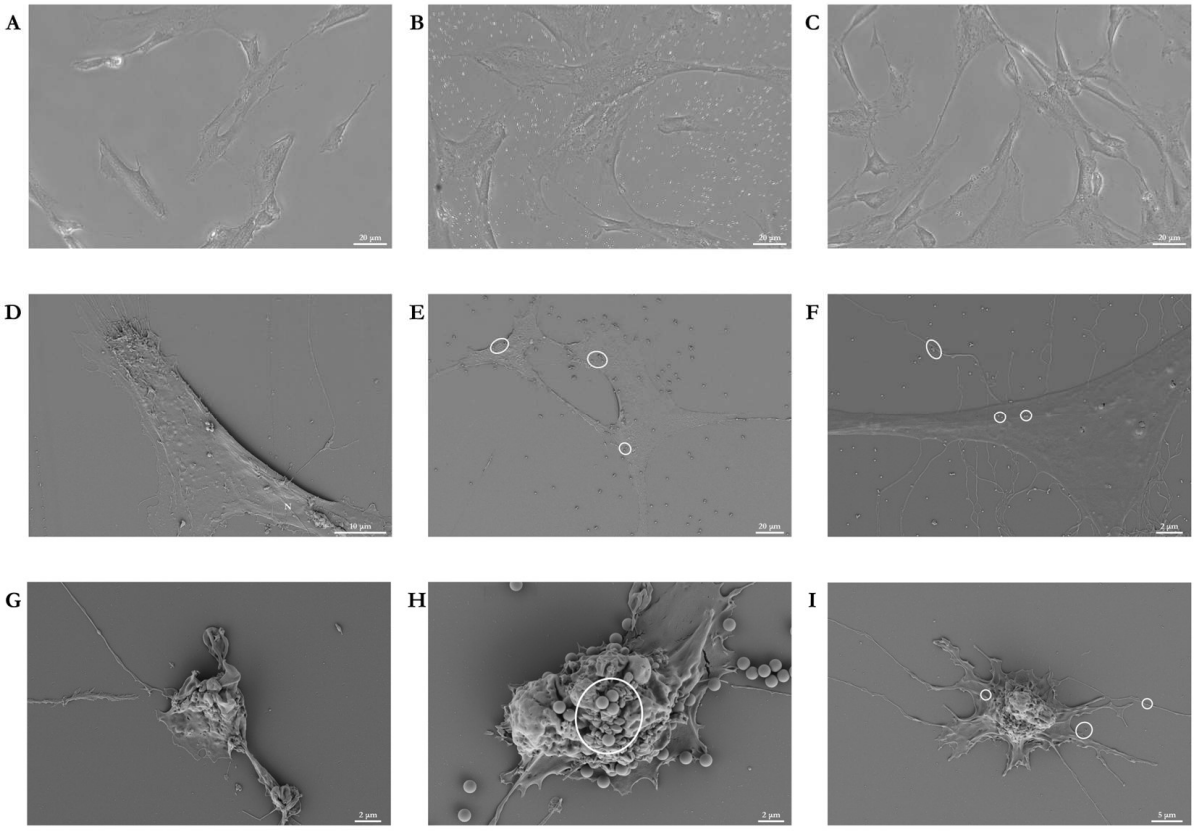

Figure 8. Representative images of cells in which endocytosis was inhibited. Phase contrast microscopy, (**A**–**C**), SEM (**D**–**I**). Control (**A**,**D**,**G**); cells exposed to $PS_{1\ \mu m}$ (**B**,**E**,**H**); cells exposed to $PS_{100\ nm}$ (**C**,**F**,**I**). As shown in panels (**E**–**H**) micro and nanoparticles are only present outside the cells (circles). N: nucleus. Scale bar 2 µm (**F**–**H**), 5 µm (**I**), 10 µm (**D**), 20 µm (**A**–**C**,**E**).

3.8. Assessment of Gene Expression After Cell Exposure to PS Particles

Expression of specific genes involved in inflammatory/immune response (IL-1β, IL-6, IL-8, TGF-β1, TNFα), oxidative stress (SOD1, CAT), and senescence (cyclin-dependent kinase inhibitor 2A-p16, Cyclin-dependent kinase inhibitor 1A-p21) was considered. Furthermore, the mRNA evaluation of stemness and differentiation markers (CD44, CD90, Alkaline Phosphatase-ALPL, Dentin Sialophosphoprotein-DSPP) was also assessed. As shown in Figure 9, from a biological perspective, exposure to $PS_{1\ \mu m}$ and $PS_{100\ nm}$ did not result in notable changes in cell mRNA expression. As the expression of TNFα, ALPL, and DSPP was very low (Ct > 35), the results were not interpretable.

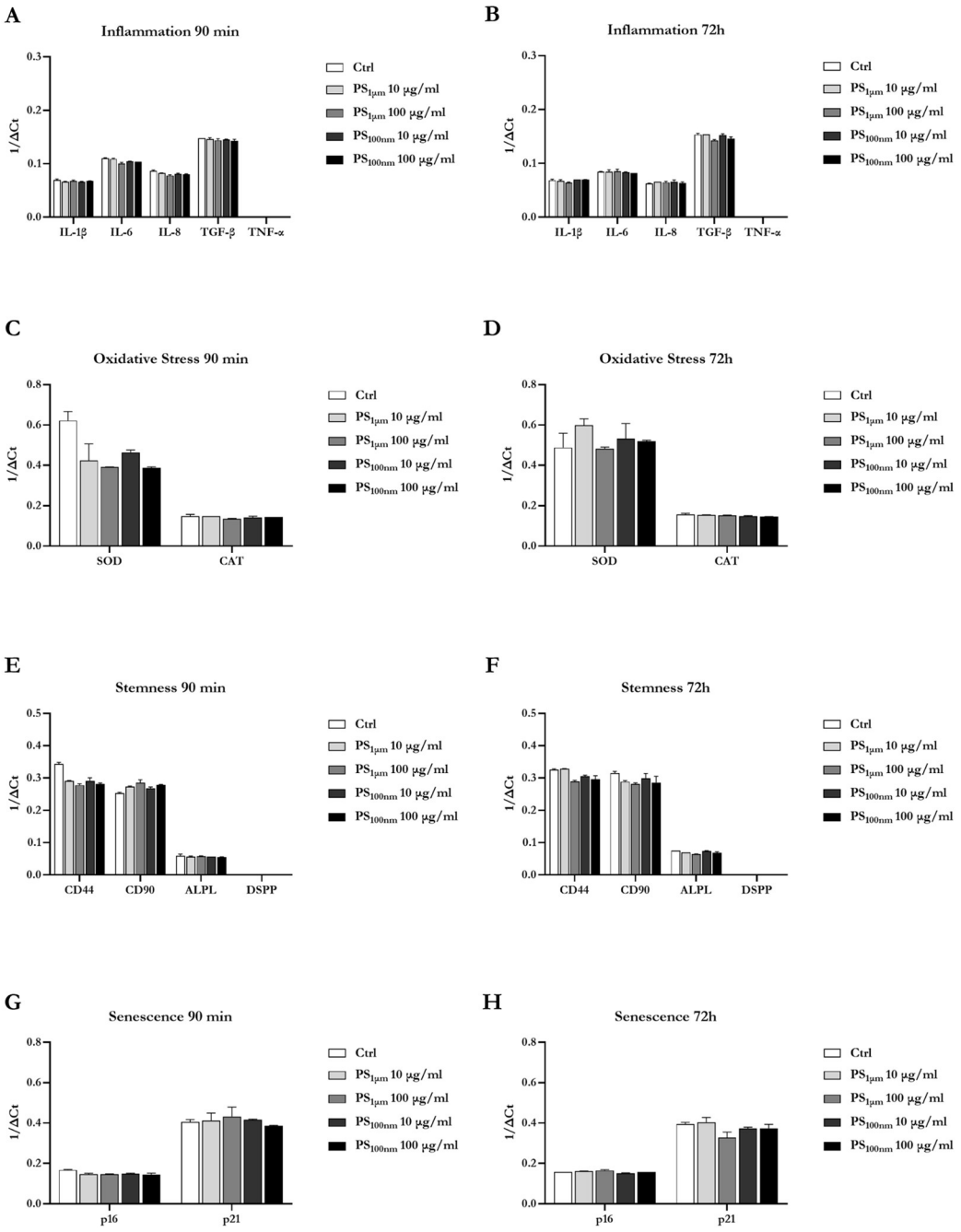

Figure 9. Real-time PCR of cells after exposure to 10 and 100 μg/mL of $PS_{1\ \mu m}$ and $PS_{100\ nm}$. Genes involved in inflammatory/immune response (**A**,**B**) (IL-1β, IL-6, IL-8, TGF-1β, TNFα), oxidative stress (**C**,**D**) (SOD1, CAT), stemness (**E**,**F**) (CD44, CD90; ALPL, DSPP) and senescence (**G**,**H**) (cyclin-dependent kinase inhibitor 2A-p16, cyclin-dependent kinase inhibitor 1A-p21) were considered. No significant differences were observed for all the studied genes.

3.9. Effect of PS Particle Aging on Gene Expression

A different pattern emerges when considering the effects of aged plastics and their dissolution media (Figure 10). Overall, the inflammatory pathway appears to be the most affected, showing a considerable increase in IL-8 after short-term exposure to aged particles (Figure 10A) and in TGF-β1 under all exposure conditions at short- and medium-term treatment (Figure 10A,B). Alterations in mRNA expression were also detected in the oxidative stress pathway, with a particularly significant decrease in SOD after short- and medium-term exposure (Figure 10C). The differentiation pathway appeared to be less

affected; only CD44 showed a decrease in mRNA level after medium-term exposure to aged $PS_{1\ \mu m}$ and to the dissolution media deriving from $PS_{100\ nm}$ particles. Regarding senescence, only p21 showed a significant increase in mRNA expression after medium-term exposure to $PS_{1\ \mu m}$ dissolution media, aged $PS_{100\ nm}$, and its respective dissolution media.

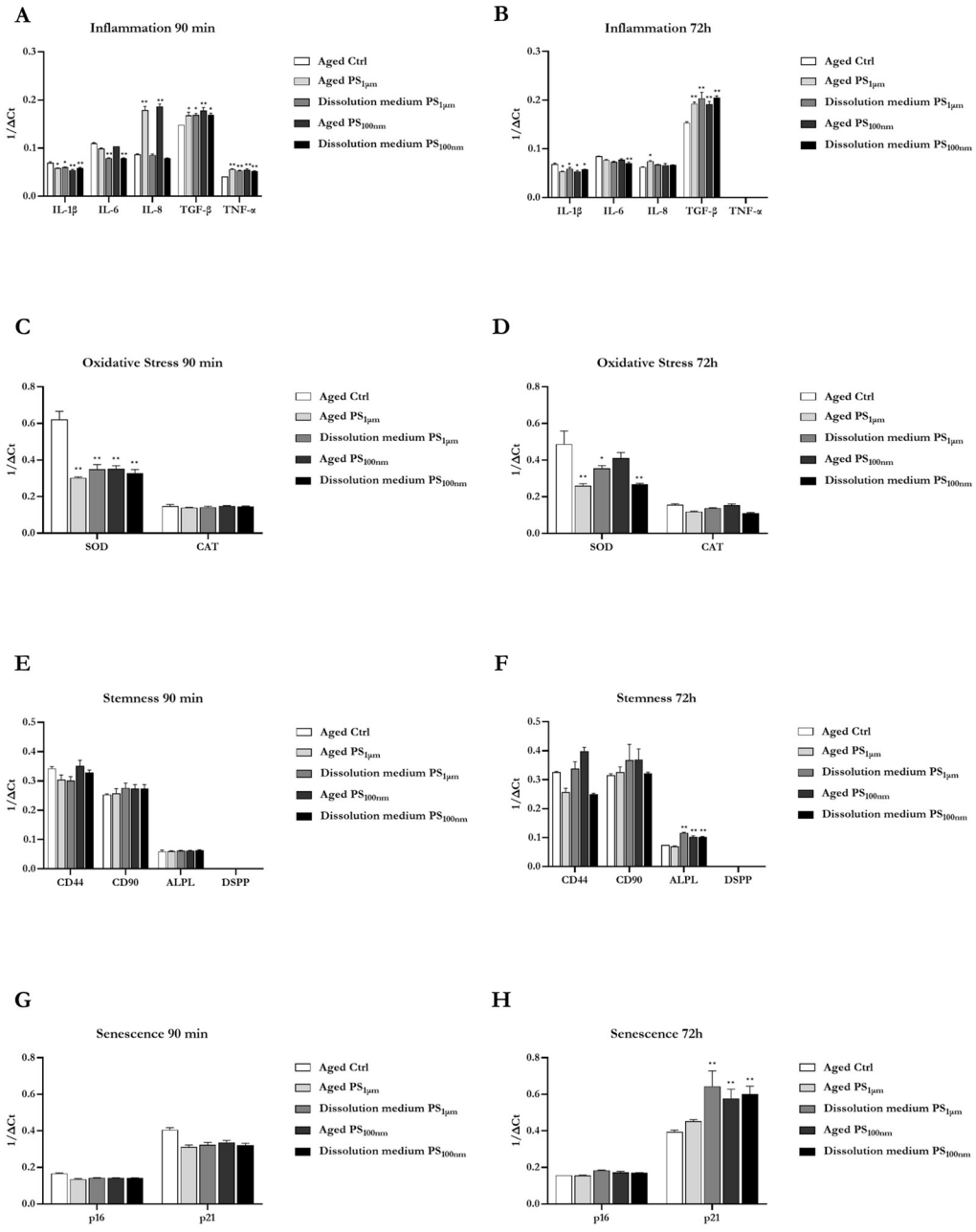

Figure 10. Real-time PCR of cells after exposure to 1 mg/mL of aged $PS_{1\ \mu m}$ and $PS_{100\ nm}$ and their dissolution medium. Genes involved in inflammatory/immune response (**A**,**B**) (IL-1β, IL-6, IL-8, TGF-1β, TNFα), oxidative stress (**C**,**D**) (SOD1, CAT), stemness (**E**,**F**) (CD44, CD90; ALPL, DSPP) and senescence (**G**,**H**) (cyclin-dependent kinase inhibitor 2A-p16, cyclin-dependent kinase inhibitor 1A-p21) was considered. Significant differences were observed for the genes involved in the inflammatory pathway, beyond SOD and ALPL. * $p < 0.01$; ** $p < 0.001$.

4. Discussion

Data on polystyrene (PS) capacities, production, consumption, and trade statistics in the recent years are provided in the comprehensive Market Research Report 2025 [38]. From the report, it is clear that the status is rather alarming, and it is also imperative to know the

long-term effects of the presence of PS in the ecosystem at the cellular level. Furthermore, prolonged daily contact with microplastics, such as those contained in food packaging, straws, beverage bottles, tea bags, paper scraps, and those released by chewing gum and teeth aligners, needs to be considered [20]. Interestingly, an average of 100 microplastic particles are released per gram of chewing gum, although some samples release up to 600 particles per gram (https://www.acs.org/pressroom/presspacs/2025 (accessed on 16 October 2025)).

Considering this framework, in this paper we investigated the susceptibility of human dental pulp stem cells (DPSCs) exposed to $PS_{1\ \mu m}$ and $PS_{100\ nm}$ in their pristine state, as well as the components leached after one month of aging in culture medium at 37 °C and 5% CO_2. This aspect is very important when studying, at the cellular level, the effects of the elements released from plastic compounds that persist in the human body following internalization.

Toxicological studies, including ours, often use higher concentrations to allow for comparison across studies and to generate robust data for risk assessment [30,33,34]. Although these concentrations exceed typical environmental levels, they are scientifically justified because they help reveal toxic effects that may not appear under chronic, low-level exposure. Higher doses also improve the detection of biological responses, clarify toxicity mechanisms, and support dose–response analysis.

Although many studies have examined the toxicological effects of PS micro- and nanoparticles, results remain inconsistent, ranging from minimal cellular effects [4,19] to marked cytotoxicity, reduced proliferation, and inflammation [18,39–41]. These discrepancies likely arise from methodological variability, including particle size and surface chemistry, dose, exposure time, aging conditions, and biological models. For example, Schmidt et al. [32,42] reported that biological outcomes depend strongly on particle size, observing only minor acute toxicity for 200-nm to 6-µm particles despite evidence of oxidative stress. Mattioda et al. [5] detected increased IL-8 expression, though their serum-free conditions are not physiologically realistic, as in vivo protein corona formation influences particle–cell interactions by promoting uptake, protecting membranes, and reducing cytotoxicity [43–45].

Several papers that used aquatic species and plants as models [46,47] are not conceptually ideal for comparison with our results. Lastly, with regard to surface chemistry, the literature reports that positively charged polystyrene (PS), particularly NH_2-PS, is more toxic than COOH-PS or non-functionalized PS [4,19]. In this scenario, it is difficult to determine whether the results we have obtained are consistent with published studies.

Even though cell viability was not highly affected by plastic particle exposure, we noticed a decrease of actomyosin cortex complexes and an increment of irregular and granular phalloidin staining, a sign of impaired actin polymerization [32,48,49]; this event could affect cell shape and adhesion.

In our experiments, uptake was substantial and mainly mediated by endocytosis, as no particles were internalized when cells were exposed to 4 °C or treated with cytochalasin D, conditions that inhibit endocytic processes [45,49,50]. SEM and phase-contrast microscopy confirmed these findings. SEM also highlighted the cytoskeletal and morphological alterations caused by cytochalasin D, including disrupted filopodia and lamellipodia, cell rounding, and reduced adhesion [51]. As shown in Figure 8G–I, cytochalasin-treated cells not only failed to internalize particles but also displayed markedly different morphology compared with cells maintained at 4 °C.

In contrast to what has been reported in the literature focused on plastic toxicity in mammalians [18,40,41], we did not observe significant biological changes in the mRNA expression of genes involved in oxidative stress, inflammation, stemness, and senescence following pristine PS exposure. Since oxidative stress and cellular senescence are closely in-

terconnected processes [52], and no changes were observed in oxidative stress-related genes in DPSCs exposed to $PS_{1\ \mu m}$ and $PS_{100\ nm}$, we did not expect alterations in senescence-associated gene expression; indeed, our results supported this assumption. Different patterns emerge when considering the effects of aged plastics and their dissolution media. Indeed, the inflammatory pathway appears to be the most affected, showing a considerable increase in IL-8 after short-term exposure to aged particles and in TGF-β1 under all exposure conditions both after short- and medium-term exposures. Undeniably, IL-8 is a key marker for assessing early inflammatory activation in many cell types, including MSCs, with a peak between 2 and 6 h after stimulation and a subsequent decrease within 24 h [53]. In addition, an increase in mRNA TGF-β1, after PS nanoplastic exposure, has been observed. Following acute damage, there is a rapid, temporary upregulation of TGF-β1 mRNA, once the inflammation subsides (2–4 days), the mRNA and protein levels return to baseline [51]. TGF-β1 is a multifunctional cytokine with a widespread expression; it can stimulate diverse cellular responses and is particularly critical to embryonic development, wound healing, and tissue and immune homeostasis. [51]. An increment of TGF-β1 after PS exposure has been reported in epithelial [54] and cardiac [55] cells, and here we have demonstrated that it occurs also in MSCs.

Although data remain limited for mammalian stem cells, in several aquatic and invertebrate models a reduced expression of SOD mRNA has been reported following exposure to micro- and/or nanoplastics, consistent with impaired cellular antioxidant capacity [56,57]. The reduced SOD mRNA expression is transient in response to a short-lived stressor, or permanent in case of severe damage [58].

Findings by other authors suggest that PS particles do not raise oxidative stress; rather, they exhibit reactive oxygen species (ROS) scavenging activity by upregulating GPX3 and downregulating HSP70 (ROS-related gene) [59]. Furthermore, Barguilla et al. [60] after 5 months of in vitro exposure of breast stem cells (MCF10A) to PS, have not identified significant changes at a functional level.

Under the tested experimental conditions, PS exposure produced minimal effects on differentiation. CD44 mRNA levels showed only a biologically insignificant decrease ($\Delta\Delta Ct < 1$) after medium-term exposure to aged $PS_{1\ \mu m}$ particles and to dissolution medium from $PS_{100\ nm}$ particles. CD90 expression remained unchanged. ALPL expression increased slightly following exposure to aged $PS_{100\ nm}$ particles and their dissolution medium. DSPP mRNA stayed undetectable. These findings partly align with Lerman et al. [61], who reported that the NH_2-PS 3D scaffold maintains stem cell proliferation without spontaneous osteogenic differentiation. Conversely, Tao et al. [62] observed that hiPSCs exposed to PS nanoplastics experienced increased cell death and reduced stem cell differentiation.

In qPCR analyses, Ct values above 35 indicate extremely low, near-limit expression and are therefore unreliable. A $\Delta\Delta Ct$ of at least 2 is required to consider a change markedly different from the normalized control. It is also essential to differentiate statistical significance from biological relevance. These criteria guided the interpretation of our data and help explain why some mRNA expression changes observed under our experimental conditions were statistically significant but not biologically meaningful.

The DPSCs used in this study were characterized by MSC markers, whose expression and proliferation rate were maintained in vitro from passage 2 to passage 30 [23]. Since prolonged in vitro culture can lead non-immortalized cells to senescence, characterized by reduced proliferation, this characteristic makes DPSCs an optimal model, especially for studying differentiation and senescence in response to xenobiotic exposure.

As also reported by other authors [4,10,19], we have found that cell viability was unaffected by exposure to plastic particles themselves, but was instead influenced by compounds leached into the culture medium. Confocal microscopy further supported this,

showing that the plastic surface changed after one month of incubation in medium. Considering the medium-term persistence of micro- and nanoplastics in both the environment and the human body, these findings warrant careful consideration. Since aging polystyrene micro- and nanoparticles can release various compounds [63] that appear to be the main drivers of cytotoxicity, we plan to chemically characterize these released substances and examine their toxicity on DPSCs in greater detail. Particular focus will be placed on styrene monomers and oligomers, and on additives such as phthalates, flame retardants, and dyes. Styrene monomers and oligomers may accumulate in lipid membranes, altering membrane phase behavior and potentially causing cell disruption [64]. Furthermore, plastic additives, being endocrine disruptors, may have negative impacts on the thyroid hormone system, erythrocytes, and the reproductive system [65–67]. The leaching of styrene-related compounds and additives from polystyrene particles raises significant concerns regarding their bioaccumulation, endocrine-disrupting potential, and overall cytotoxic effects, underscoring the need for thorough toxicological evaluation, particularly in sensitive cell systems such as DPSCs. To further elucidate the nature and concentration of the leached compounds, future experiments will employ advanced analytical chemistry techniques, such as gas chromatography–mass spectrometry and liquid chromatography–mass spectrometry. These methods will enable the identification and quantification of organic compounds released from plastic debris under physiological conditions. Additionally, time-course studies will be conducted to evaluate the kinetics of compound release over extended incubation periods. Integrating this chemical profiling with biological assays will provide a more comprehensive understanding of the potential risks that micro- and nanoplastics pose to human health.

With this work, we believe we have added a small but valuable contribution to current knowledge, aimed at better understanding the mechanisms of plastic toxicity at the cellular level. Additionally, our study seeks to raise public awareness about the risks associated with the excessive production, use, and disposal of plastics in the environment.

5. Conclusions

Plastic is highly resistant to degradation and can persist in the environment for hundreds of years, accumulating in ecosystems and entering the food chain as micro- and nanoplastics. These tiny particles not only pose a serious threat to wildlife and biodiversity but can also be internalized by humans. Once inside the body, they may cross physiological barriers and release harmful compounds that interact with cells over time, potentially leading to chronic health effects. Among the many concerns is their impact on cellular systems crucial to human health, such as those responsible for tissue repair and regeneration. However, studies on their cytotoxicity in humans, especially at the microscopic scale, remain limited. Investigating their effects through cellular models, including stem cells, is therefore crucial for understanding both ecological and human health risks.

This study examined the effects of PS micro- and nanoparticles on human DPSCs, focusing on both pristine and aged particles. While pristine PS did not significantly affect cell viability or alter gene expression related to oxidative stress, inflammation, stemness, or senescence, aged PS leachates reduced viability, indicating that toxicity likely arises from released chemical components. Impaired actin polymerization and altered cell morphology were observed despite maintained cell survival. PS particles were actively internalized via endocytosis. These findings highlight the importance of considering particle aging and leachate composition in toxicity assessments. DPSCs, characterized by stable stem cell markers and proliferation over multiple passages, proved to be a valuable model for such studies, and this work underscores the importance of stem cell-based toxicological assessments to better understand human cellular responses to plastic pollutants. Overall,

this work underscores the complex nature of plastic toxicity and the need for further research into the chemical and biological impacts of microplastics in human systems.

Supplementary Materials: The following supporting information can be downloaded at: https://www.mdpi.com/article/10.3390/microplastics5010025/s1.

Author Contributions: Conceptualization, supervision, writing original draft preparation, manuscript revision, and funding acquisition: R.G.; formal analysis, methodology, data analysis and figure drafting: L.B., F.R., M.B. and M.R.; investigation: R.P.; manuscript revision: M.M. and T.C.; investigation, review and editing and funding acquisition: C.P.; data curation review and editing and funding acquisition: G.B. All authors have read and agreed to the published version of the manuscript.

Funding: This research was funded by University of Insubria, Fondo Comune di Ateneo per la Ricerca (FAR_2023) to R.G., G.B., C.P.

Institutional Review Board Statement: The study was conducted in accordance with the Declaration of Helsinki, and approved by the Ethics Committee Ospedale di Circolo Fondazione Macchi (Protocol number: 0034066, approval date: 3 October 2013).

Informed Consent Statement: Informed consent was obtained from the subject's legal guardians involved in the study.

Data Availability Statement: The original contributions presented in this study are included in the article and Supplementary Material. Further inquiries can be directed to the corresponding author.

Acknowledgments: The authors are grateful to Piero Antonio Zecca of the University of Insubria for providing the dental pulp used for DPSC extraction. Scientific support from CRIETT center of University of Insubria (instrument code MIC02) is greatly acknowledged. We thank Bengt Fadeel, Karolinska Institutet, for insightful comments on the manuscript.

Conflicts of Interest: The authors declare no conflicts of interest.

References

1. Nisha; Joshi, H.C. A Systematic Review: Biodegradation, Mechanism, Remediation Strategies, and Environmental Impacts of Microplastics. *Asia-Pac. J. Chem. Eng.* **2024**, *19*, e3122. [CrossRef]
2. Kik, K.; Bukowska, B.; Sicińska, P. Polystyrene Nanoparticles: Sources, Occurrence in the Environment, Distribution in Tissues, Accumulation and Toxicity to Various Organisms. *Environ. Pollut.* **2020**, *262*, 114297. [CrossRef]
3. Kwon, B.G.; Koizumi, K.; Chung, S.-Y.; Kodera, Y.; Kim, J.-O.; Saido, K. Global Styrene Oligomers Monitoring as New Chemical Contamination from Polystyrene Plastic Marine Pollution. *J. Hazard. Mater.* **2015**, *300*, 359–367. [CrossRef]
4. Banerjee, A.; Billey, L.O.; Shelver, W.L. Uptake and Toxicity of Polystyrene Micro/Nanoplastics in Gastric Cells: Effects of Particle Size and Surface Functionalization. *PLoS ONE* **2021**, *16*, e0260803. [CrossRef]
5. Mattioda, V.; Benedetti, V.; Tessarolo, C.; Oberto, F.; Favole, A.; Gallo, M.; Martelli, W.; Crescio, M.I.; Berio, E.; Masoero, L.; et al. Pro-Inflammatory and Cytotoxic Effects of Polystyrene Microplastics on Human and Murine Intestinal Cell Lines. *Biomolecules* **2023**, *13*, 140. [CrossRef] [PubMed]
6. Vo, H.C.; Pham, M.H. Ecotoxicological Effects of Microplastics on Aquatic Organisms: A Review. *Environ. Sci. Pollut. Res.* **2021**, *28*, 44716–44725. [CrossRef]
7. Jalaudin Basha, N.N.; Adzuan Hafiz, N.B.; Osman, M.S.; Abu Bakar, N.F. Unveiling the Noxious Effect of Polystyrene Microplastics in Aquatic Ecosystems and Their Toxicological Behavior on Fishes and Microalgae. *Front. Toxicol.* **2023**, *5*, 1135081. [CrossRef]
8. Kelpsiene, E.; Ekvall, M.T.; Lundqvist, M.; Torstensson, O.; Hua, J.; Cedervall, T. Review of Ecotoxicological Studies of Widely Used Polystyrene Nanoparticles. *Environ. Sci. Process. Impacts* **2022**, *24*, 8–16. [CrossRef] [PubMed]
9. Hwang, J.; Choi, D.; Han, S.; Jung, S.Y.; Choi, J.; Hong, J. Potential Toxicity of Polystyrene Microplastic Particles. *Sci. Rep.* **2020**, *10*, 7391. [CrossRef] [PubMed]
10. Paul, M.B.; Fahrenson, C.; Givelet, L.; Herrmann, T.; Loeschner, K.; Böhmert, L.; Thünemann, A.F.; Braeuning, A.; Sieg, H. Beyond Microplastics–Investigation on Health Impacts of Submicron and Nanoplastic Particles after Oral Uptake In Vitro. *Microplastics Nanoplastics* **2022**, *2*, 16. [CrossRef]
11. Saud, S.; Yang, A.; Jiang, Z.; Ning, D.; Fahad, S. New Insights in to the Environmental Behavior and Ecological Toxicity of Microplastics. *J. Hazard. Mater. Adv.* **2023**, *10*, 100298. [CrossRef]

12. Issac, M.N.; Kandasubramanian, B. Effect of Microplastics in Water and Aquatic Systems. *Environ. Sci. Pollut. Res.* **2021**, *28*, 19544–19562. [CrossRef] [PubMed]
13. Siddiqui, S.A.; Singh, S.; Bahmid, N.A.; Shyu, D.J.H.; Domínguez, R.; Lorenzo, J.M.; Pereira, J.A.M.; Câmara, J.S. Polystyrene Microplastic Particles in the Food Chain: Characteristics and Toxicity—A Review. *Sci. Total Environ.* **2023**, *892*, 164531. [CrossRef]
14. Zaini, N.; Kasmuri, N.; Mojiri, A.; Kindaichi, T.; Nayono, S.E. Plastic Pollution and Degradation Pathways: A Review on the Treatment Technologies. *Heliyon* **2024**, *10*, e28849. [CrossRef]
15. Landrigan, P.J.; Raps, H.; Cropper, M.; Bald, C.; Brunner, M.; Canonizado, E.M.; Charles, D.; Chiles, T.C.; Donohue, M.J.; Enck, J.; et al. The Minderoo-Monaco Commission on Plastics and Human Health. *Ann. Glob. Health* **2023**, *89*, 23. [CrossRef]
16. van Emmerik, T.H.M.; Kirschke, S.; Schreyers, L.J.; Nath, S.; Schmidt, C.; Wendt-Potthoff, K. Estimating Plastic Pollution in Rivers through Harmonized Monitoring Strategies. *Mar. Pollut. Bull.* **2023**, *196*, 115503. [CrossRef]
17. Geremia, E.; Muscari Tomajoli, M.T.; Murano, C.; Petito, A.; Fasciolo, G. The Impact of Micro- and Nanoplastics on Aquatic Organisms: Mechanisms of Oxidative Stress and Implications for Human Health—A Review. *Environments* **2023**, *10*, 161. [CrossRef]
18. He, T.; Qu, Y.; Yang, X.; Liu, L.; Xiong, F.; Wang, D.; Liu, M.; Sun, R. Research Progress on the Cellular Toxicity Caused by Microplastics and Nanoplastics. *J. Appl. Toxicol.* **2023**, *43*, 1576–1593. [CrossRef]
19. Jeon, M.S.; Kim, J.W.; Han, Y.B.; Jeong, M.H.; Kim, H.R.; Sik Kim, H.; Park, Y.J.; Chung, K.H. Polystyrene Microplastic Particles Induce Autophagic Cell Death in BEAS-2B Human Bronchial Epithelial Cells. *Environ. Toxicol.* **2022**, *38*, 359–367. [CrossRef]
20. Ma, C.; Ramachandraiah, K.; Jiang, G. Micro and Nano Plastics: Contaminants in Beverages and Prevention Strategies. *Front. Sustain. Food Syst.* **2024**, *8*, 1491290. [CrossRef]
21. Yu, C.; Abbott, P. An Overview of the Dental Pulp: Its Functions and Responses to Injury. *Aust. Dent. J.* **2007**, *52*, S4–S6. [CrossRef]
22. Barone, L.; Gallazzi, M.; Rossi, F.; Papait, R.; Raspanti, M.; Zecca, P.A.; Buonarrivo, L.; Bassani, B.; Bernardini, G.; Bruno, A.; et al. Human Dental Pulp Mesenchymal Stem Cell-Derived Soluble Factors Combined with a Nanostructured Scaffold Support the Generation of a Vascular Network In Vivo. *Nanomaterials* **2023**, *13*, 2479. [CrossRef] [PubMed]
23. Barone, L.; Cucchiara, M.; Palano, M.T.; Bassani, B.; Gallazzi, M.; Rossi, F.; Raspanti, M.; Zecca, P.A.; De Antoni, G.; Pagiatakis, C.; et al. Dental Pulp Mesenchymal Stem Cell (DPSCs)-Derived Soluble Factors, Produced under Hypoxic Conditions, Support Angiogenesis via Endothelial Cell Activation and Generation of M2-like Macrophages. *J. Biomed. Sci.* **2024**, *31*, 99. [CrossRef]
24. Li, B.; Ouchi, T.; Cao, Y.; Zhao, Z.; Men, Y. Dental-Derived Mesenchymal Stem Cells: State of the Art. *Front. Cell Dev. Biol.* **2021**, *9*, 654559. [CrossRef]
25. Cherubino, M.; Valdatta, L.; Balzaretti, R.; Pellegatta, I.; Rossi, F.; Protasoni, M.; Tedeschi, A.; Accolla, R.S.; Bernardini, G.; Gornati, R. Human Adipose-Derived Stem Cells Promote Vascularization of Collagen-Based Scaffolds Transplanted into Nude Mice. *Regen. Med.* **2016**, *11*, 261–271. [CrossRef] [PubMed]
26. Conrad, C.; Huss, R. Adult Stem Cell Lines in Regenerative Medicine and Reconstructive Surgery. *J. Surg. Res.* **2005**, *124*, 201–208. [CrossRef] [PubMed]
27. Borgese, M.; Rossi, F.; Bonfanti, P.; Colombo, A.; Mantecca, P.; Valdatta, L.; Bernardini, G.; Gornati, R. Recovery Ability of Human Adipose Stem Cells Exposed to Cobalt Nanoparticles: Outcome of Dissolution. *Nanomedicine* **2020**, *15*, 453–465. [CrossRef]
28. Papis, E.; Rossi, F.; Raspanti, M.; Dalle-Donne, I.; Colombo, G.; Milzani, A.; Bernardini, G.; Gornati, R. Engineered Cobalt Oxide Nanoparticles Readily Enter Cells. *Toxicol. Lett.* **2009**, *189*, 253–259. [CrossRef]
29. Gornati, R.; Pedretti, E.; Rossi, F.; Cappellini, F.; Zanella, M.; Olivato, I.; Sabbioni, E.; Bernardini, G. Zerovalent Fe, Co and Ni Nanoparticle Toxicity Evaluated on SKOV-3 and U87 Cell Lines. *J. Appl. Toxicol.* **2016**, *36*, 385–393. [CrossRef]
30. Gheorghe, Ş.; Pătraşcu, A.-M.; Stoica, C.; Balas, M.; Feodorov, L. Ecotoxicological Effects of Polystyrene Particle Mix (20, 200, and 430 Mm) on Cyprinus Carpio. *Toxics* **2025**, *13*, 246. [CrossRef]
31. Palombella, S.; Pirrone, C.; Cherubino, M.; Valdatta, L.; Bernardini, G.; Gornati, R. Identification of Reference Genes for qPCR Analysis during hASC Long Culture Maintenance. *PLoS ONE* **2017**, *12*, e0170918. [CrossRef] [PubMed]
32. Schmidt, A.; Da Silva Brito, W.A.; Singer, D.; Mühl, M.; Berner, J.; Saadati, F.; Wolff, C.; Miebach, L.; Wende, K.; Bekeschus, S. Short- and Long-Term Polystyrene Nano- and Microplastic Exposure Promotes Oxidative Stress and Divergently Affects Skin Cell Architecture and Wnt/Beta-Catenin Signaling. *Part. Fibre Toxicol.* **2023**, *20*, 3. [CrossRef]
33. Wang, X.; Jian, S.; Zhang, S.; Wu, D.; Wang, J.; Gao, M.; Sheng, J.; Hong, Y. Enrichment of Polystyrene Microplastics Induces Histological Damage, Oxidative Stress, Keap1-Nrf2 Signaling Pathway-Related Gene Expression in Loach Juveniles (*Paramisgurnus dabryanus*). *Ecotoxicol. Environ. Saf.* **2022**, *237*, 113540. [CrossRef]
34. Yedier, S.; Yalçınkaya, S.K.; Bostancı, D. Exposure to Polypropylene Microplastics via Diet and Water Induces Oxidative Stress in Cyprinus Carpio. *Aquat. Toxicol.* **2023**, *259*, 106540. [CrossRef] [PubMed]
35. Mäger, I.; Langel, K.; Lehto, T.; Eiríksdóttir, E.; Langel, Ü. The Role of Endocytosis on the Uptake Kinetics of Luciferin-Conjugated Cell-Penetrating Peptides. *Biochim. Biophys. Acta (BBA)-Biomembr.* **2012**, *1818*, 502–511. [CrossRef]
36. Rossi, F.; Bernardini, G.; Bonfanti, P.; Colombo, A.; Prati, M.; Gornati, R. Effects of TCDD on Spermatogenesis Related Factor-2 (SRF-2): Gene Expression in Xenopus. *Toxicol. Lett.* **2009**, *191*, 189–194. [CrossRef]

37. Gronthos, S.; Mankani, M.; Brahim, J.; Robey, P.G.; Shi, S. Postnatal Human Dental Pulp Stem Cells (DPSCs) in Vitro and in Vivo. *Proc. Natl. Acad. Sci. USA* **2000**, *97*, 13625–13630. [CrossRef]
38. Research and Markets. *Polystyrene (PS) World, Regions and Countries Market Analysis 2019–2024 and Outlook to 2034*; Market Reasearch Report; Research and Markets: Birmingham, UK, 2025; p. 205.
39. Guanglin, L.; Shuqin, W. Polystyrene Nanoplastics Exposure Causes Inflammation and Death of Esophageal Cell. *Ecotoxicol. Environ. Saf.* **2024**, *269*, 115819. [CrossRef]
40. Saenen, N.D.; Witters, M.S.; Hantoro, I.; Tejeda, I.; Ethirajan, A.; Van Belleghem, F.; Smeets, K. Polystyrene Microplastics of Varying Sizes and Shapes Induce Distinct Redox and Mitochondrial Stress Responses in a Caco-2 Monolayer. *Antioxidants* **2023**, *12*, 739. [CrossRef] [PubMed]
41. Wang, X.; Ren, X.-M.; He, H.; Li, F.; Liu, K.; Zhao, F.; Hu, H.; Zhang, P.; Huang, B.; Pan, X. Cytotoxicity and Pro-Inflammatory Effect of Polystyrene Nano-Plastic and Micro-Plastic on RAW264.7 Cells. *Toxicology* **2023**, *484*, 153391. [CrossRef]
42. Schmidt, A.; Mühl, M.; Brito, W.A.D.S.; Singer, D.; Bekeschus, S. Antioxidant Defense in Primary Murine Lung Cells Following Short- and Long-Term Exposure to Plastic Particles. *Antioxidants* **2023**, *12*, 227. [CrossRef]
43. Brouwer, H.; Porbahaie, M.; Boeren, S.; Busch, M.; Bouwmeester, H. The in Vitro Gastrointestinal Digestion-Associated Protein Corona of Polystyrene Nano- and Microplastics Increases Their Uptake by Human THP-1-Derived Macrophages. *Part. Fibre Toxicol.* **2024**, *21*, 4. [CrossRef] [PubMed]
44. Janke, U.; Geist, N.; Weilbeer, E.; Levin, W.; Delcea, M. Impact of Protein Corona Formation and Polystyrene Nanoparticle Functionalisation on the Interaction with Dynamic Biomimetic Membranes Comprising of Integrin. *ChemBioChem* **2024**, *25*, e202400188. [CrossRef]
45. Kihara, S.; Ashenden, A.; Kaur, M.; Glasson, J.; Ghosh, S.; van der Heijden, N.; Brooks, A.E.S.; Mata, J.P.; Holt, S.; Domigan, L.J.; et al. Cellular Interactions with Polystyrene Nanoplastics—The Role of Particle Size and Protein Corona. *Biointerphases* **2021**, *16*, 041001. [CrossRef] [PubMed]
46. Wu, J.; Liu, W.; Zeb, A.; Lian, J.; Sun, Y.; Sun, H. Polystyrene Microplastic Interaction with Oryza Sativa: Toxicity and Metabolic Mechanism. *Environ. Sci. Nano* **2021**, *8*, 3699–3710. [CrossRef]
47. Zhang, Q.; Wang, F.; Xu, S.; Cui, J.; Li, K.; Shiwen, X.; Guo, M. Polystyrene Microplastics Induce Myocardial Inflammation and Cell Death via the TLR4/NF-κB Pathway in Carp. *Fish Shellfish. Immunol.* **2023**, *135*, 108690. [CrossRef] [PubMed]
48. Pugnaloni, A.; Lucarini, G.; Giantomassi, F.; Lombardo, L.; Capella, S.; Belluso, E.; Zizzi, A.; Panico, A.M.; Biagini, G. In Vitro Study of Biofunctional Indicators after Exposure to Asbestos-like Fluoro-Edenite Fibres. *Cell. Mol. Biol.* **2007**, *53*, 965–980.
49. DeLoid, G.M.; Yang, Z.; Bazina, L.; Kharaghani, D.; Sadrieh, F.; Demokritou, P. Mechanisms of Ingested Polystyrene Micro-Nanoplastics (MNPs) Uptake and Translocation in an in Vitro Tri-Culture Small Intestinal Epithelium. *J. Hazard. Mater.* **2024**, *473*, 134706. [CrossRef]
50. Yang, C.; Colosi, P.; Hugelier, S.; Zabezhinsky, D.; Lakadamyali, M.; Svitkina, T. Actin Polymerization Promotes Invagination of Flat Clathrin-Coated Lattices in Mammalian Cells by Pushing at Lattice Edges. *Nat. Commun.* **2022**, *13*, 6127. [CrossRef]
51. Deng, Z.; Fan, T.; Xiao, C.; Tian, H.; Zheng, Y.; Li, C.; He, J. TGF-β Signaling in Health, Disease and Therapeutics. *Signal Transduct. Target. Ther.* **2024**, *9*, 61. [CrossRef]
52. Mahmud, F.; Sarker, D.B.; Jocelyn, J.A.; Sang, Q.-X.A. Molecular and Cellular Effects of Microplastics and Nanoplastics: Focus on Inflammation and Senescence. *Cells* **2024**, *13*, 1788. [CrossRef]
53. Van Gorp, H.; Van Opdenbosch, N.; Lamkanfi, M. Inflammasome-Dependent Cytokines at the Crossroads of Health and Autoinflammatory Disease. *Cold Spring Harb. Perspect. Biol.* **2019**, *11*, a028563. [CrossRef]
54. Michelini, S.; Mawas, S.; Kurešepi, E.; Barbero, F.; Šimunović, K.; Miremont, D.; Devineau, S.; Schicht, M.; Ganin, V.; Haugen, Ø.P.; et al. Pulmonary Hazards of Nanoplastic Particles: A Study Using Polystyrene in in Vitro Models of the Alveolar and Bronchial Epithelium. *J. Nanobiotechnol.* **2025**, *23*, 388. [CrossRef]
55. Lin, P.; Tong, X.; Xue, F.; Qianru, C.; Xinyu, T.; Zhe, L.; Zhikun, B.; Shu, L. Polystyrene Nanoplastics Exacerbate Lipopolysaccharide-Induced Myocardial Fibrosis and Autophagy in Mice via ROS/TGF-B1/Smad. *Toxicology* **2022**, *480*, 153338. [CrossRef]
56. Arini, A.; Muller, S.; Coma, V.; Grau, E.; Sandre, O.; Baudrimont, M. Origin, Exposure Routes and Xenobiotics Impart Nanoplastics with Toxic Effects on Freshwater Bivalves. *Environ. Sci. Nano* **2023**, *10*, 1352–1371. [CrossRef]
57. Ranjan, H.; Senthil Kumar, S.; Priscilla, S.; Swaminathan, S.; Umezawa, M.; Sheik Mohideen, S. Polyethylene Microplastics Affect Behavioural, Oxidative Stress, and Molecular Responses in the *Drosophila* Model. *Environ. Sci. Process. Impacts* **2024**, *26*, 2203–2214. [CrossRef] [PubMed]
58. Niu, C.-S.; Chang, C.-K.; Lin, L.-S.; Jou, S.-B.; Kuo, D.-H.; Liao, S.-S.; Cheng, J.-T. Modification of Superoxide Dismutase (SOD) mRNA and Activity by a Transient Hypoxic Stress in Cultured Glial Cells. *Neurosci. Lett.* **1998**, *251*, 145–148. [CrossRef] [PubMed]
59. Im, G.-B.; Kim, Y.G.; Jo, I.-S.; Yoo, T.Y.; Kim, S.-W.; Park, H.S.; Hyeon, T.; Yi, G.-R.; Bhang, S.H. Effect of Polystyrene Nanoplastics and Their Degraded Forms on Stem Cell Fate. *J. Hazard. Mater.* **2022**, *430*, 128411. [CrossRef]
60. Barguilla, M.-S.V.; Guyot, B. Stem Cells as Unique Models to Study Long-Term Effects Triggered by Micro- and Nanoplastic Exposure: A Focus on Cell Transformation and Differentiation. *Span. J. Environ. Mutagen. Genom.* **2023**, *27*, 141.

61. Lerman, M.J.; Smith, B.T.; Gerald, A.G.; Santoro, M.; Fookes, J.A.; Mikos, A.G.; Fisher, J.P. Aminated 3D Printed Polystyrene Maintains Stem Cell Proliferation and Osteogenic Differentiation. *Tissue Eng. Part C Methods* **2020**, *26*, 118–131. [CrossRef] [PubMed]
62. Tao, M.; Wang, C.; Zheng, Z.; Gao, W.; Chen, Q.; Xu, M.; Zhu, W.; Xu, L.; Han, X.; Guo, X.; et al. Nanoplastics Exposure-Induced Mitochondrial Dysfunction Contributes to Disrupted Stem Cell Differentiation in Human Cerebral Organoids. *Ecotoxicol. Environ. Saf.* **2024**, *285*, 117063. [CrossRef] [PubMed]
63. Gulizia, A.M.; Patel, K.; Philippa, B.; Motti, C.A.; van Herwerden, L.; Vamvounis, G. Understanding Plasticiser Leaching from Polystyrene Microplastics. *Sci. Total Environ.* **2023**, *857*, 159099. [CrossRef]
64. Morandi, M.I.; Kluzek, M.; Wolff, J.; Schroder, A.; Thalmann, F.; Marques, C.M. Accumulation of Styrene Oligomers Alters Lipid Membrane Phase Order and Miscibility. *Proc. Natl. Acad. Sci. USA* **2021**, *118*, e2016037118. [CrossRef]
65. Arrigo, F.; Impellitteri, F.; Piccione, G.; Faggio, C. Phthalates and Their Effects on Human Health: Focus on Erythrocytes and the Reproductive System. *Comp. Biochem. Physiol. Part. C Toxicol. Pharmacol.* **2023**, *270*, 109645. [CrossRef]
66. Bereketoglu, C.; Pradhan, A. Plasticizers: Negative Impacts on the Thyroid Hormone System. *Environ. Sci. Pollut. Res.* **2022**, *29*, 38912–38927. [CrossRef] [PubMed]
67. Paramasivam, A.; Murugan, R.; Jeraud, M.; Dakkumadugula, A.; Periyasamy, R.; Arjunan, S. Additives in Processed Foods as a Potential Source of Endocrine-Disrupting Chemicals: A Review. *J. Xenobiotics* **2024**, *14*, 1697–1710. [CrossRef] [PubMed]